Thermally Actuated Rotary Type Micro Actuator with Curved Beams

M. Arefin Anwar[1], M. Packirisamy[2] and and A. K. W. Ahmed[3]
Optical Microsystems Laboratory, CONCAVE Research Center,
Department Of Mechanical and Industrial Engineering, Concordia University,
1455 de Maisonneuve Blvd. West, Montreal, Quebec H3G 1M8, Canada

ABSTRACT

This paper presents a novel rotary type micro thermal actuator with curved hot arm that provides in plane rotary motion of the cold disc. Performance of an actuator with curved hot segment and circular disc shaped cold arm is investigated. Upon application of potential difference between cold and hot segments, the cold disc rotates about its center and this rotary motion can be useful for various optical MEMS applications such as, switching, attenuation, diffraction, etc. The device was fabricated by MUMPS technology. A Finite Element Method (FEM) analysis on the actuator was done by defining air volume around the structure followed by the substrate. A mathematical model was used to predict the thermo-mechanical behavior of the thermal actuator and was validated by comparing with the results obtained from FEM.

Keywords: Optical MEMS, rotary type micro thermal actuator

1. INTRODUCTION

Electrostatic and electro thermal actuators are the most common actuators available in micro dimension. Electrostatic actuators provide limited displacement and force on the other hand, electro thermal actuators provide larger force and deflection. More over, thermal actuators can be fabricated by Integrated Circuit (IC) compatible surface micromachining technology [1, 2]. As a result, micro thermal actuator finds wide applications and is under constant exploration for new applications. This paper presents a thermal actuator with new structural topology. Upon application of voltage, the narrower segment called hot arm is heated due to Joule heating and the wider section called the cold disc works as a heat sink in combination with the surrounding. It results in asymmetrical thermal expansion of hot arms and makes the cold disc rotate. The thermal actuator was fabricated in Multi- USER MEMS Processes (MUMPS) technology [3].

The thermal boundary conditions of a micro thermal actuator, depends on the fabrication process [4]. For a micro thermal actuator fabricated in MUMPS technology, the dominant modes of heat transfer in the operating range are lateral conduction through the structure and vertical conduction through the gap between the structure and the substrate [5, 6]. Convection and radiation heat transfer are ignored for the same reasons [5, 7]. Lott et al. [8] used a finite difference approach for solving the heat transfer of a chevron type micro thermal actuator and validated with analytical approach [7]. This paper considers conductions as the main mode of heat transfer and ignores convection and radiation. A simplified mathematical model was used for design purpose. A FEM analysis was done and the simplified model was validated by comparing the results with that of FEM analysis.

2. ACTUATOR DESIGN

Shown in Fig. 1, is the thermal actuator with a set of hot arms placed on the opposite sides of the cold disc in such a way that the cold disc will work as moment arm. This unique arrangement makes the disc to rotate upon application of voltage. The proposed actuator has a circular disc at the center which acts as a sink or cold segment. The disc is attached to the anchors through highly flexural curved beams, called hot arms or hot segments. Both the hot arms and cold disc are made from the same

[1] M.A.Sc. Candidate, arefinanwar@yahoo.com
[2] Assistant Professor, pmuthu@vax2.concordia.ca, Tel: (514) 848-2424 Ext. 7973
[3] Professor, waiz@vax2.concordia.ca, Tel: (514) 848-2424 Ext. 7932

polysilicon layer of MUMPS process. As the polysilicon is a piezoresistive material, the hot arms have very high electrical resistance when compared to cold disc. The main intent of the present design are to have large relative thermal expansion between hot and cold segments, very flexible hot arms and smaller foot-print of the device. Hence the design is proposed with curved hot arms in this paper in order to meet the said constraints. One could achieve longer hot arm leading to high thermal expansion by making it curved between the disc and anchors while keeping the distance between them as constant.

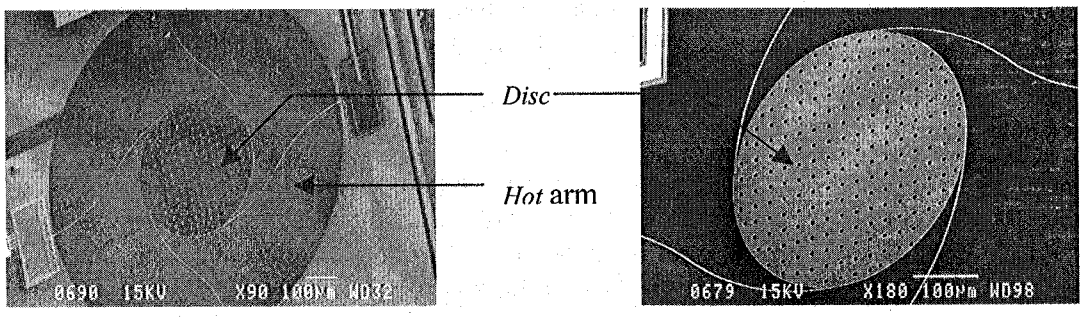

(a) (b)

Figure 1: (a) Scanning Electron Micrograph (SEM) of the novel rotary type micro thermal actuator fabricated in MUMPS technology & (b): Close up SEM of the cold disc

In order to make the device structurally stable and stronger, hot arms are symmetrically distributed around the disc as shown in Fig. 1. The flexural longitudinal stiffness of the hot arms is very much dependent on the boundary support conditions. If one end of the hot arm is free, then one would expect maximum longitudinal expansion at the free end. But the presence of the rigid cold disc at the end introduces compressive load on the arms leading to transverse motion of the beam in addition to the longitudinal expansion. The ratio of the longitudinal expansion to the lateral or transverse motion is dependent on the size of the disc. As the purpose of this paper is to demonstrate the feasibility of the novel actuator, free expansion is assumed for hot arms for simplicity.

3. THERMAL ANALYSIS

Among the four anchor pads of the thermal actuator, two are used to apply voltage and the other two are made as ground. Because of the symmetry in the hot beams, a pair of the beams along with the cold disc was considered. A simplified one dimensional heat transfer analysis is employed for analyzing a micro thermal actuator [5, 7, 8, 9]. In this paper, a Finite Difference Method (FDM) analysis is presented that considers one dimensional heat transfer and this method can also provide transient temperature distribution of the thermal actuator until it reaches steady state. In the FDM method, the device along its length is divided into discrete nodes spaced by equal distance Δx and each node is assigned an elemental volume of Δu. Properties of a specific element is represented by the corresponding node. In this analysis, curved beams were modeled as straight beams of same arc length.

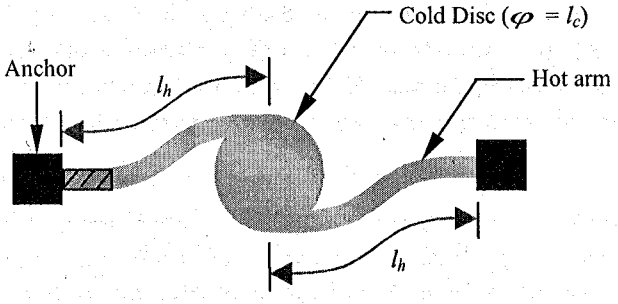

(a)

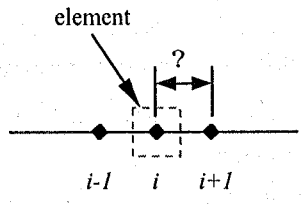

(c)

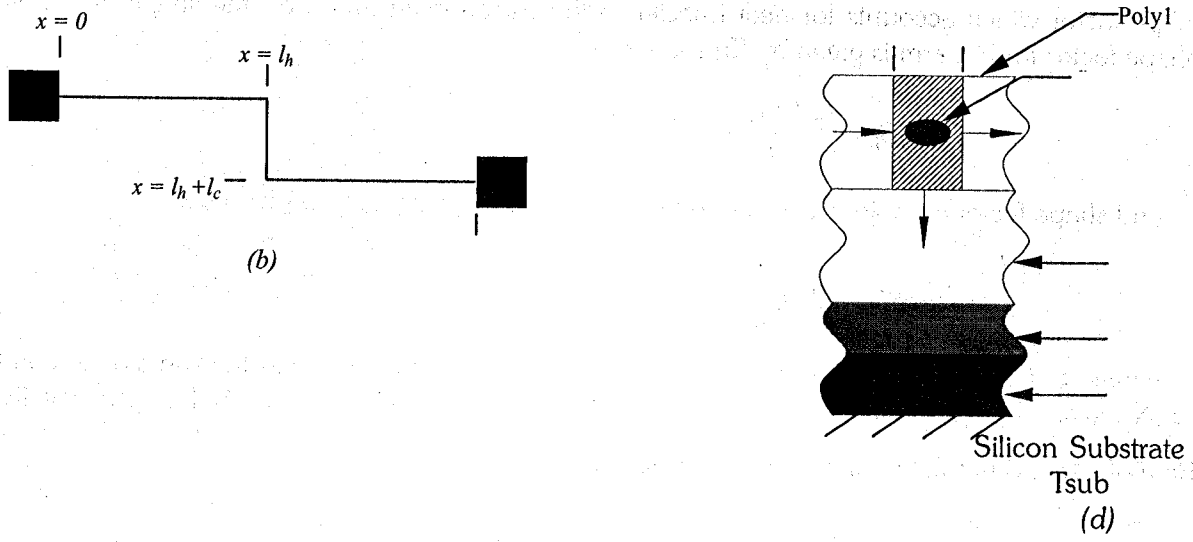

Figure 2: (a)Schematic rotary type micro thermal actuator, (b) simplified coordinate system, (c) representation of FDM nodal system along the length of the actuator and (d) Heat transfer modes involved in ith element of micro thermal actuator

In Fig. 2, l_h is the arc length of a hot arm and l_c is the diameter of a cold disc. Energy balance for ith node yields following algebraic relation:

$$q_{joule} + q_{i-1} - q_{i+1} - q_{out,\,sub} = q \tag{1}$$

where, q_{joule} is the rate of energy generated in ith element by joule heating, q_{i-1} is the rate of heat input to the ith element from *i-1*th element, q_{i+1} is the rate of heat output from ith element to the next element, $q_{out,\,sub}$ accounts for heat transferred to the surrounding from ith element and q is the rate of heat accumulation in the element. Solving this equation for all the nodes in the structure yields nodal temperatures.

Rate of heat generation due to joule heating can be approximated as,

$$q_{joule} = J^2 \rho_r \Delta u_i \tag{2}$$

where, J is the current density in a given element, ρ_r is the temperature dependent resistivity and Δu_i is the element volume. Current density can be approximated as,

$$J_h = \frac{I}{w_h t_p} \text{ and } J_c = \frac{2I}{w_c t_p} \tag{3}$$

where, the subscripts h and c stands for hot arm and cold disc respectively, w is the width of any given element and t_p is the thickness. I is the passing current through any given element. For calculating current density of cold disc, $2I$ is considered in order to account for the presence of another pair of hot arms. Width of cold disc is approximated from the length of a side of an equivalent square area [9].

Lateral conduction between nodes, *i-1* and i is given by,

$$q_{i-1} = \frac{k_p A_c}{Dx}\left[T_{i-1}(k) - T_i(k)\right] \tag{4}$$

where, A_c is cross sectional area at any ith node, k_p is thermal conductivity of polysilicon and Δx is the distance between the nodes. In this literature, $T_i(k)$ will represent the temperature of ith node at kth time. There is a time increment of Δt between each time step.

$$q_{out,sub} = \frac{SA_s}{R_T}\left[T_i(k) - T_{sub}\right] \tag{5}$$

where, T_{sub} is the temperature of the substrate, A_s represents surface area of the element which is in parallel to the substrate, R_T is the thermal resistance between the structure and the substrate and S is the

shape factor which accounts for heat transfer to the surrounding based on the shape of the element. Shape factor for hot arm is given by [5] as,

$$S_h = \frac{t_p}{w_h}\left(\frac{2t_a}{t_p}+1\right)+1 \tag{6}$$

and shape factor for cold disc is found later. Thermal resistance, R_T is given by,

$$R_T = \frac{t_a}{k_a} + \frac{t_{p0}}{k_{p0}} \quad \frac{t_n}{k_n} \tag{7}$$

where, t_a, t_{p0} and t_n are the thickness of air, thickness of Poly0 layer and thickness of Silicon Nitride (Si_3N_4) layer and k_a, k_{p0} and k_n are the thermal conductivity of air, Poly0 and Si_3N_4, respectively.

Rate of heat accumulation in the node is calculated from,

$$q = \frac{\rho c \Delta u_i}{\Delta t}\left[T_i(k+1) - T_i(k)\right] \tag{8}$$

where, ρ and c are the density and specific heat of polysilicon respectively. Resistivity is assumed as a function of temperature and can be expressed as,

$$\rho_r = \rho_o\left[1+\xi(T_i(k-1) - T_{sub})\right] \tag{9}$$

where, ξ is linear temperature co-efficient of resistivity.

Substituting Eqn (2)-(8) into Eqn (1), an explicit expression for the temperature at time $k+1$, in terms of temperatures at time k, the input and the boundary conditions can be formed as,

$$T_i(k+1) = \frac{\Delta t}{\rho c \Delta u_i}\left[J^2(k)\rho_r \Delta u_i + \frac{SA_s}{R_T}(T_{sub} - T_i(k)) + \frac{k_p A_c}{\Delta x}(T_{i-1}(k) - T_i(k)) + \frac{k_p A_c}{\Delta x}(T_{i+1}(k) - T_i(k))\right] + T_i(k) \tag{10}$$

Solving Equation (10) with proper initial and boundary conditions, the temperature of any element at any given time step can be found through out the structure. As per the initial conditions, room temperature will prevail through out the structure at 20°C. For the subsequent thermal boundary conditions, anchors are assumed to be constrained at room temperature of 20°C, due to the bulk heat capacity of substrate.

When the steady state is reached, average temperature of a hot arm can be measured and used to measure the thermal expansion of the free end of the beam as follows:

$$\Delta L_h = \alpha l_h (T_{avg} - T_{sub}) \tag{11}$$

where, α is the co-efficient of thermal expansion and T_{avg} is the average temperature of a hot arm.

4. ROTATIONAL ANALYSIS

To measure the rotation of disc, a cantilever analogy was used, i.e., one end is free to move. Thermal expansion of the beam is calculated using average temperature of a beam and this angle of rotation was estimated using the following simplified formula [9],

$$\Delta L_h = R\theta \tag{12}$$

where, θ is the angle of rotation and R is the radius of the disc

In order to demonstrate that thermal actuator with curved beam provides more rotation than a thermal actuator with straight beam in a given foot-print of radius of periphery, $R_p = 673\mu m$, the following Model1 and Model 2 as shown in Fig.3 were investigated and the corresponding results are shown in Fig. 7.

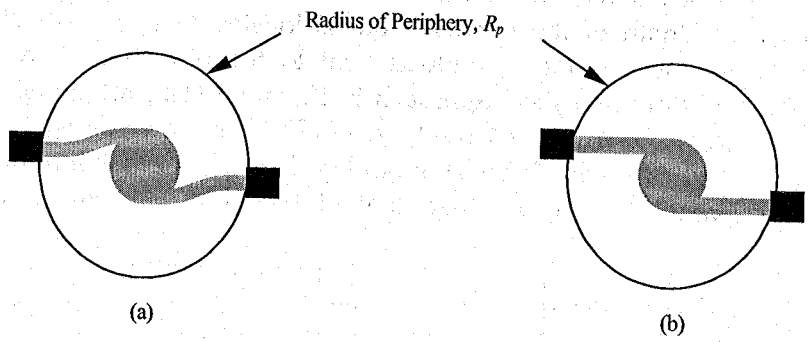

Figure 3: (a) Model 1, Schematic of rotary type micro thermal actuator with curved beam, (b) Model 2, Schematic of rotary type micro thermal actuator with straight beams

Table 1: Models used for the analysis

Model	l_h (μm)	R (μm)	R_p (μm)
1	732	250	673
2	625	250	673

Table1: Parameters used for the analysis [10]

Parameter	Value
Elastic Modulus of polysilicon (E)	169 GPa
Poisson's ratio polysilicon (γ)	0.22
Coefficient of thermal expansion of polysilicon (α)	$2.7\text{x}10^{-6}\text{K}^{-1}$
Electrical resistivity of polysilicon at room temperature (ρ_0)	$2\text{x}10^{-3}$ Ω-cm
Resistivity co-efficient of polysilicon (ξ)	$1.25\text{x}10^{-3}\ ^{\circ}\text{K}^{-1}$
Thermal conductivity of poly1 (k_p)	32 $\text{W-m}^{-1}\text{-}^{\circ}\text{K}^{-1}$
Thermal conductivity of poly0 (k_{p0})	32 $\text{W-m}^{-1}\text{-}^{\circ}\text{K}^{-1}$
Thermal conductivity of air (k_a)	0.026 $\text{W-m}^{-1}\text{-}^{\circ}\text{K}^{-1}$
Thermal conductivity of nitride (k_n)	2.25 $\text{W-m}^{-1}\text{-}^{\circ}\text{K}^{-1}$
Thickness of Poly1, t_p	2 μm
Thickness of air, t_a	2 μm
Thickness of Poly0, t_{p0}	0.5 μm
Thickness of Nitride, t_n	0.6 μm

5. FINITE ELEMENT ANALYSIS

FEM analysis of the device was done in ANSYS 8.1. In the FEM model, an air volume was defined from the level of top surface of the structure followed with Poly0 layer and nitride layer. Since convection heat transfer is negligible and radiation is significant only at high temperature, the air layer on top of the structure was not defined [9]. A coupled field element, Solid98 was used for meshing the structure and thermal element, Solid87 was used for meshing the surrounding layers. In this model, anchor pads were constrained for motions in all directions and at room temperature of T_{sub}=20°C. The bottom surface of nitride layer was constrained at room temperature of T_{sub}=20°C. Electrical potential was applied between two anchor pads and the other two anchor pads were made as ground. For rotation measurement of the disc, slope of an imaginary line connecting two diametrically opposite nodes, before and after applying loads, were used.

6. RESULTS AND DISCUSSIONS

Temperature distribution obtained from analytical approach was compared with that from the FEM. By best matching the temperature distribution of the cold disc of Model1 [9], a shape factor for the disc was found as 0.35. Using this new shape factor, steady state temperature distribution of Model1 from analytical approach, was found to be close to that from FEM as shown in Fig. 4. Also, average temperature of a hot arm of Model1 from both methods were compared and it was found that average tempera-

ture from analytical approach was slightly higher than that of FEM results as shown in Fig. 5. This is due to the fact that a significant length of the curved beam is located with in very close proximity of the large sized cold disc and as a result it conducts heat to the disc through air. Substituting the average temperature obtained from analytical approach in Equation (12), rotational behavior of cold disc of Model1 was computed and found to be close to that of FEM as shown in Fig. 6. The comparison shown in Fig. 6 thus validates the presented model. From Fig. 7, it is evident that rotation of the cold disc is more in Model 1 with curved beam than that of Model 2 with straight beam.

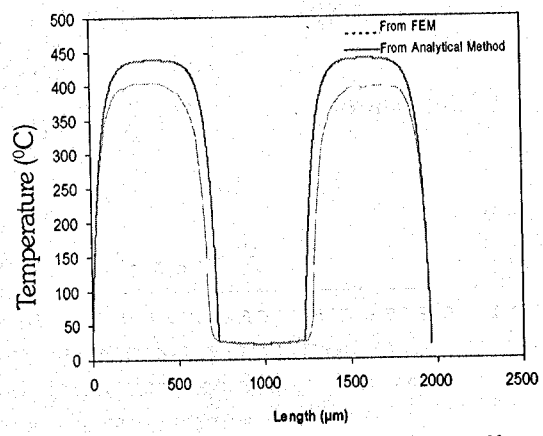

Figure 4: Steady state Temperature profile of Model1 obtained from FEM and Analytical method, at 3.1004m-A.

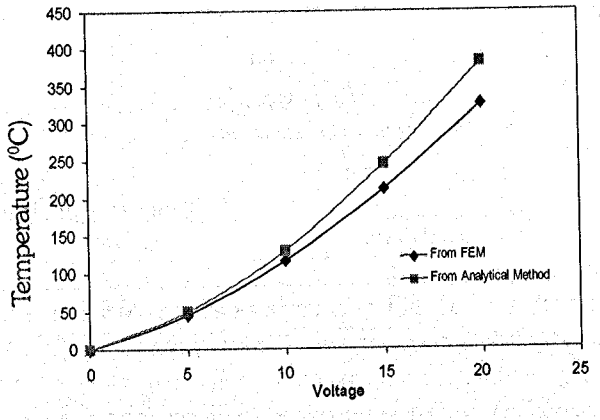

Figure 5: Average temperature of a hot arm of Model1, obtained from both analytical approach and FEM at different applied voltages

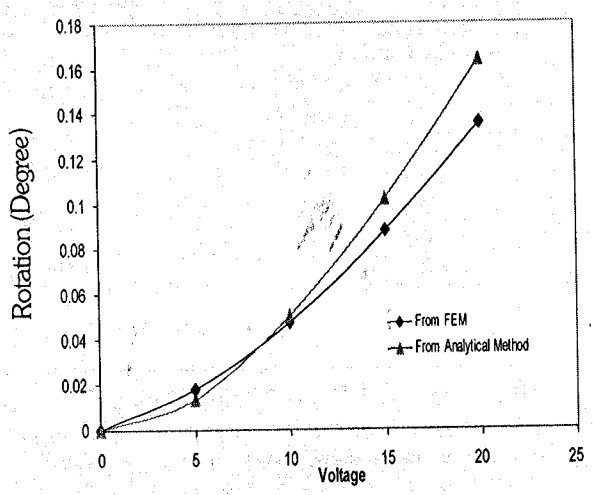

Figure 6: Rotational behavior (in degree) of the cold disc of Model1, obtained from both analytical approach and FEM at different applied voltages

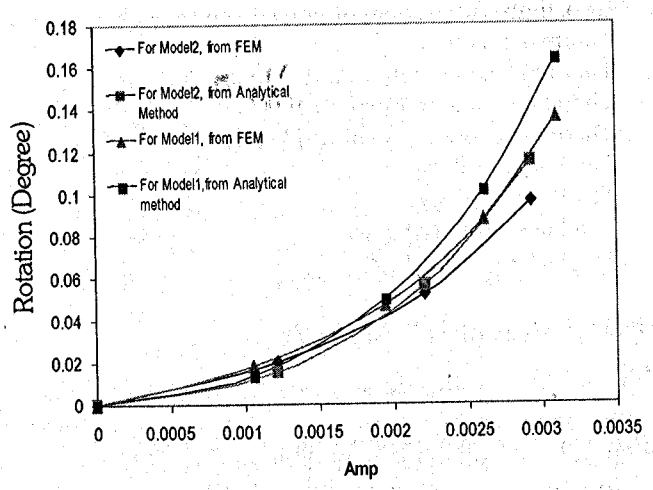

Figure 7: Comparison of rotational behavior (in degree) of Model 1 & Model 2 as a function of input current

7. CONCLUSION

Curved beam thermal actuators can be beneficial than the straight beam actuators for increased rotation under space constraints. The comparison of the analytical approach with FEM shows close agreement and validates the model. The presented results also confirm the applicability of this novel rotary type micro thermal actuator for various optical applications such as, switching, diffraction, attenuation etc.

Acknowledgement

Authors would like to acknowledge the support of Canadian Microelectronics Corporation (CMC) and National Science and Engineering Research Council of Canada (NSERC).

References:

1. Comtois, J. H., Bright, V. M., Applications for surface-micromachined polysilicon thermal actuator and arrays, Sensors and Actuators A, vol.58, pp. 19-25, 1997.
2. Pan, C.S., HSU, W., An electro-thermally and laterally driven polysilicon. micro actuator, Journal of Micromechanics and Microengineering, vol. 7, pp.7-13, 1997.
3. Koester, D. A., Mahadevan, R., Hardy, B., Markus and K. W., MUMPS Design Handbook, Cronos Integrated Microsystems, JDS Uniphase, Revision 7.0, 2001
4. Mankame, N. D. and Ananthasuresh, G. K., Comprehensive thermal modeling and characterization of an electro-thermal-complaint microactuator, Journal of Micromechanics and Microengineering, vol. 11, pp. 1-11, 2001
5. Lin, L., Chiao, M., Electrothermal responses of lineshape microstructures, Sensors and Actuators A, vol. 55, pp. 35-41, 1996.
6. Hickey, R., Analysis and Optimal Design of Micro-Machined Thermal Actuators, M.A.Sc. Thesis, Dalhousie University, Nova Scotia, Canada, 2001.
7. Huang, Q. A., Lee, N. K. S., Analysis and design polysilicon thermal flexure actuator, Journal of Micromechanics and Microengineering, vol. 9, pp. 64-70, 1999.
8. Lott, C. D., McLain, T. W., Harb, J. N. and Howell, L. L., Modeling the thermal behavior of a surface-micromachined linear displacement thermomechanical microactuator, Sensors and Actuators A, vol. 101, pp. 239-250, 2002
9. Anwar, M. Arefin, Packirisamy, Muthukumaran and Ahmed, A. K. Waiz, Electro thermal analysis of rotary type micro thermal actuator, SPIE-Photonics North '2005 proceedings, 5907A_41
10. Atre, A. and Boedo, S., Effect of Thermophysical property variations on surface micromachined polysilicon beam flexure actuator, NSTI-Nanotech 2004, vol. 2, pp. 263-266, 2004

——— • • • ———